

# UC San Diego

## UC San Diego Previously Published Works

### Title

Role of Curcuminoids and Tricalcium Phosphate Ceramic in Rat Spinal Fusion

### Permalink

<https://escholarship.org/uc/item/7fd1948z>

### Journal

Tissue Engineering Part C Methods, 26(11)

### ISSN

1937-3384

### Authors

Ryan, Daniel A  
Cheng, Jiongjia  
Masuda, Koichi  
[et al.](#)

### Publication Date

2020-11-01

### DOI

10.1089/ten.tec.2020.0217

Peer reviewed

**METHODS ARTICLE**

---

# Role of Curcuminoids and Tricalcium Phosphate Ceramic in Rat Spinal Fusion

Daniel A. Ryan, PhD,<sup>1</sup> Jiongjia Cheng, PhD,<sup>1</sup> Koichi Masuda, MD,<sup>2</sup> and John R. Cashman, PhD<sup>1</sup>

Despite considerable research effort, there is a significant need for safe agents that stimulate bone formation. Treatment of large or complex bone defects remains a challenge. Implantation of small molecule-induced human bone marrow-derived mesenchymal stromal cells (hBMSCs) on an appropriate tricalcium phosphate (TCP) scaffold offers a robust system for noninvasive therapy for spinal fusion. To show the efficacy of this approach, we identified a small molecule curcuminoid that when combined with TCP ceramic in the presence of hBMSCs selectively induced growth of bone cells: after 8- or 25-day incubations, alkaline phosphatase was elevated. Treatment of hBMSCs with curcuminoid 1 and TCP ceramic increased osteogenic target gene expression (i.e., *Runx2*, *BMP2*, *Osteopontin*, and *Osteocalcin*) over time. In the presence of curcuminoid 1 and TCP ceramic, osteogenesis of hBMSCs, including proliferation, differentiation, and mineralization, was observed. No evidence of chondrogenic or adipogenic potential using this protocol was observed. Transplantation of curcuminoid 1-treated hBMSC/TCP mixtures into the spine of immunodeficient rats showed that it achieved spinal fusion and provided greater stability of the spinal column than untreated hBMSC-TCP implants or TCP alone implants. On the basis of histological analysis, greater bone formation was associated with curcuminoid 1-treated hBMSC implants manifested as contiguous growth plates with extensive hematopoietic territories. Stimulation of hBMSCs by administration of small molecule curcuminoid 1 in the presence of TCP ceramic afforded an effective noninvasive strategy that increased spinal fusion repair and provided greater stability of the spinal column after 8 weeks in immunodeficient rats.

**Keywords:** bone marrow-derived mesenchymal stem cells, curcumins, tricalcium phosphate ceramic, bone growth

## Impact Statement

Bone defects only slowly regenerate themselves in humans. Current procedures to restore spinal defects are not always effective. Some have side effects. In this article, a new method to produce bone growth within 8 weeks in rats is presented. In the presence of tricalcium phosphate ceramic, curcuminoid-1 small molecule-stimulated human bone marrow-derived mesenchymal stromal cells showed robust bone cell growth *in vitro*. Transplantation of this mixture into the spine showed efficient spinal fusion in rats. The approach presented herein provides an efficient biocompatible scaffold for delivery of a potentially clinically useful system that could be applicable in patients.

## Introduction

**D**ESPITE SUCCESS OF bone grafts, treatment of large or complex bone defects remains a challenge.<sup>1</sup> Autograft bone harvest limitations include prolonged recovery time, increased surgical blood loss, and pain.<sup>2</sup> Use of autologous bone may be compromised by underlying bone or metabolic

disorders that limit patient eligibility. Allografts may be applicable to individuals with underlying conditions, but allograft comes with safety concerns.<sup>3</sup> Alternatively, osteo-inductive bioceramics can be used as graft substitutes to stimulate bone formation.<sup>4</sup> Bioceramics overcome disadvantages of autografts and allografts because ceramics are not derived from human tissue. Human bone marrow-derived

---

<sup>1</sup>Human BioMolecular Research Institute, San Diego, California, USA.

<sup>2</sup>Department of Orthopedic Surgery, University of California, San Diego, San Diego, California, USA.

mesenchymal stromal cells (hBMSCs) represent another approach. hBMSC-based therapy can provide exogenous cells in bone repair and regeneration.<sup>5,6</sup>

hBMSCs play a fundamental role in bone biology and osteogenesis.<sup>7</sup> hBMSCs can differentiate into osteoblasts, adipocytes, or chondrocytes.<sup>8</sup> hBMSCs are considered “immune privileged” because hBMSCs repress recipient T cells. Implantation of allogeneic hBMSCs does not lead to host immune rejection<sup>9</sup> nor develop MHC-Class II receptors.<sup>10</sup> hBMSCs can be isolated from allogeneic sources, culture expanded, and transplanted into humans without host immune rejection. hBMSCs produce cytokines and trophic factors that modulate adjacent cells and affect their functional activity, immune response, and differentiation.<sup>11</sup> Accordingly, allogeneic hBMSCs have been investigated clinically.<sup>12</sup>

Recombinant bone morphogenetic proteins (BMPs) are used as scaffold modifiers for bone grafts,<sup>13</sup> but safety concerns have emerged.<sup>14</sup> Small molecules that mimic functions of endogenous growth factors to stimulate stem cell self-renewal or differentiation<sup>15,16</sup> have been developed that stimulate differentiation of osteoblasts from hBMSCs<sup>17–20</sup> or potentiate effects of BMP2 on hBMSCs.<sup>21</sup> However, it is yet to be shown if a small molecule approach can directly stimulate bone growth *in vivo*. New osteogenic agents are desired, and safe methods for integration with currently practiced bone repair interventions are needed.

Herein, we show that small molecules and an osteoinductive tricalcium phosphate (TCP) ceramic can be used together to induce hBMSC osteogenic lineage commitment in a cell-based therapy. Safe, small-molecule osteogenic curcuminoids afforded hBMSC osteogenesis.<sup>22,23</sup> Curcumin was reported to increase rat MSC differentiation into osteoblasts *in vitro* when added to osteogenic medium.<sup>24</sup> To date, minor curcuminoids (e.g., bisdemethoxycurcumin, BDC) and synthetic curcumin derivatives have not been examined in osteogenesis.

Herein, water-soluble prodrugs of BDC (1) and synthetic curcuminoid (2) showed potent osteogenesis. Compound 1 and 2 incubated with hBMSCs, and osteoinductive TCP showed potent effects on hBMSC osteogenic differentiation. Compound 1-induced hBMSC-TCP implants afforded significant osteoinductivity using an intramuscular implant model in immunodeficient rats and showed that small-molecule osteogenic agent induced hBMSCs in the presence of a ceramic cell carrier are of great utility as a cell-based therapy for bone growth and repair.

## Materials and Methods

### Compounds

Curcumins, including bisdemethoxy curcumin di-L-valinyl ester dihydrochloride salt, 1, were prepared<sup>25–29</sup> and purity was >95%.<sup>28,29</sup> TCP ceramic (0.5–1.0 mm granule composition) was determined by XRD to be 95/5 TCP/hydroxyapatite.<sup>4,30</sup> TCP was provided by Dr. Tim Moseley (NuVasive). TCP was sterilized by  $\gamma$ -irradiation before use. TCP scaffolds were sheets of TCP:collagen (88%:12%), see the Supplementary Data.

### Cell culture

hBMSCs were provided by Dr. Pam Robey of the NIH Center for Regenerative Medicine (Bethesda, MD). hBMSCs were

cultured in Dulbecco's modified Eagle medium (DMEM) containing 20% fetal bovine serum (FBS) and  $1 \times$  GlutaMAX.<sup>31</sup>

### Alkaline phosphatase activity

hBMSCs were cultured at a density of 1800 hBMS cells/cm<sup>2</sup> for 8 days in 12-well plates with test compounds + TCP (5 mg/mL). Cells were lysed and alkaline phosphatase (ALP) activity determined.<sup>32</sup>

### Quantification of gene expression by qPCR

hBMSCs were cultured the same as that in the ALP studies. Total RNA was extracted using TRIzol (Life Technologies). Quantitative polymer chain reaction (qPCR) (Supplementary Table S1) was run as previously described.<sup>32</sup>

### Cell viability

hBMSCs were seeded at a density of 500 cells/well in 96-well plates and grown for 24 h before adding test compounds + TCP (5 mg/mL). Cell viability was measured using an Alamar Blue assay.

### Cell staining

Alizarin Red S staining was modified from a kit (Millipore). Oil Red O (ORO) was stained for the presence of adipocytes (0.5% stock solution in isopropanol and diluted to 0.03% in deionized water). Alcian Blue was stained for the presence of chondrocytes (1% wt/v in 3% acetic acid, pH 2.5). Cell culture incubations were as described above for ALP studies.

### Apoptosis

hBMSCs were incubated with 1 or 2 (500 nM) for 25 days. Apoptosis biomarkers *Bax* and *c-Fos* mRNA quantification was done by qPCR.

### In vivo studies

Twenty-one male 10-week-old immunodeficient rats (200 g, Taconic Biosciences) were used in this study. Rats were purchased and housed at UC San Diego. All experiments were conducted with the approval of the IACUC committees of HBRI and UCSD. After anesthesia, rats were euthanized, and L4-L5 spinal fusion implants were removed and subjected to constant bending forces and visually ranked by blinded trained observers as described in the Supplementary Data.

Three groups of nude rats were used as follows: (A) DMEM on TCP scaffold, (B) untreated hBMSCs placed on TCP scaffold, and (C) 1-treated (500 nM) hBMSCs placed on TCP scaffold. Early passage hBMSCs ( $\leq 5$  passages) were seeded (density of 17,500 cells/well in six-well plates) and cultured for 24 h before cell induction. For groups B and C, hBMSCs were then cultured for 8 days with TCP granules (5 mg/mL) or in the case of group C, TCP granules (5 mg/mL) + 1 (500 nM) before implantation in immunodeficient rats. For hBMSC induction (i.e., group C), 1 (500 nM) was added on day 0, and media replenished every 48 h with 1 (500 nM) until day 8. After 8 days, cells were harvested and separated from TCP granules by centrifugation. For implantation, cell samples were placed on the precut TCP scaffold before implantation.

On the day of surgery, implants containing (A) 200  $\mu$ L DMEM and Tisseel (10  $\mu$ L of Tisseel component A

containing 0.16 mg/ $\mu$ L fibrinogen, ASD) placed on TCP scaffold, (B) 0.7 million untreated hBMSCs combined with 200  $\mu$ L DMEM and Tisseel placed on TCP scaffold, or (C) 1-induced (500 nM) hBMSCs (0.7 million) combined with 200  $\mu$ L DMEM and Tisseel and placed on TCP scaffold were prepared and kept cold (4°C). Tisseel component B (10  $\mu$ L containing 0.036 mg/ $\mu$ L thrombin) was added to each implant. TCP scaffold alone or cell scaffold with Fibrin gel was immediately used for implantation.

Rats received implants of: (A) TCP scaffold alone ( $n=7$  rats, 14 implants), (B) untreated hBMSCs on TCP scaffold ( $n=7$ , 14 implants), and (C) implants of 1-treated hBMSCs on TCP scaffold ( $n=7$ , 14 implants). Each week for 8 weeks, rats were analyzed with imaging.<sup>30</sup> At 8 weeks, rats were evaluated by computed tomography for spinal fusion<sup>31</sup> and, thereafter, euthanized. Rat spines containing implants were subjected to constant bending force analysis and visually ranked by blinded trained observers.  $\mu$ CT images of L4-L5 vertebral disc height measurements were used for determining stability of the lumbar spinal segments under controlled lateral displacement. Distance of left length and right length of L4-L5 disc height was determined by  $\mu$ CT at the neutral position and then under a constant left ( $\pm 10$  mm) and right ( $-10$  mm) lateral displacement. Deviation in disc height was calculated from the averaged differences in disc height from the neutral position that represented the absolute

sum of contraction and elongation deviations. Implants were harvested and immediately fixed in 10% neutral buffered formalin as described in the Supplementary Data.

### Statistical analysis

Statistical analysis was done with GraphPad Prism showing the mean and standard deviation (SD) or standard error of mean (SEM) of at least triplicate samples for each biological assay. Student *t*-tests were used for pairwise comparisons.  $p < 0.05$  was considered significant. \*  $p < 0.05$ , \*\*  $p < 0.01$ , \*\*\*  $p < 0.001$ . In some cases, other statistical treatments were used.

## Results

### Stimulation of hBMSC osteogenesis by curcumins

Bisdemethoxycurcumin 3 (BDC), a minor curcuminoid of turmeric (5–10%), and curcumin 4 (Curc), a major curcuminoid (65–80%) and amino acid conjugates 1 and 2 that increased the water solubility and stability of curcumins (Fig. 1A–C), were independently prepared (Supplementary Data). Curcumins (i.e., 500 nM) stimulated hBMSC osteogenesis based on ALP activity.<sup>31</sup> ALP activity was linearly dependent on concentration of curcumins up to 500 nM. A measure of 500 nM was chosen for further studies,

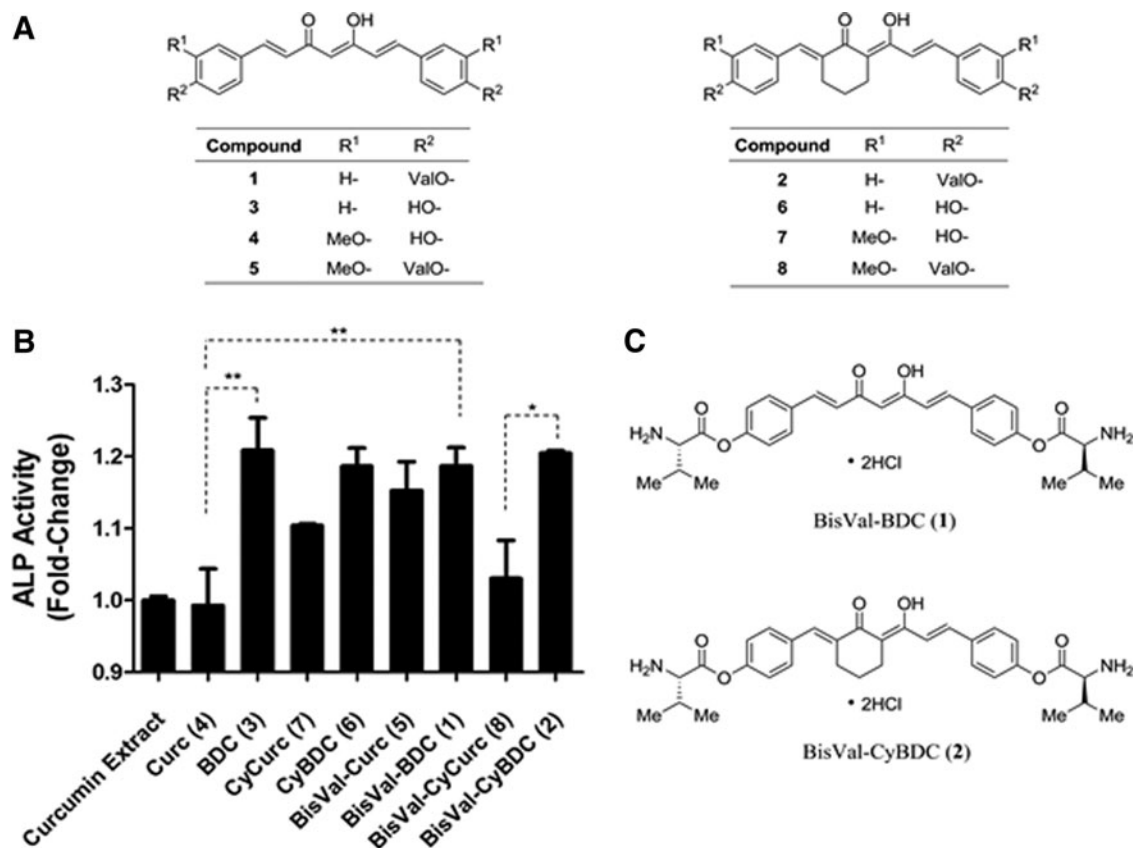


**FIG. 1.** Naturally-occurring and synthetic curcumins tested for ALP activity in hBMSC osteogenic differentiation. (A) Curcumins synthesized and tested for osteogenic differentiation. (B) Effect of curcumins 1–8 (500 nM) and curcumin extract (500 nM, weighted average concentration of curcumins) on ALP activity after an 8-day incubation with hBMSCs. Data are mean fold-change ALP activity  $\pm$  SD ( $n=3$ ) normalized to turmeric extract. \* $p < 0.05$ , \*\* $p < 0.01$ . (C) Shows compounds 1 and 2 selected for advanced studies. ALP, alkaline phosphatase; hBMSC, human bone marrow-derived mesenchymal stromal cell.

and significant differences in hBMSC ALP activity were observed after 8 days (Fig. 1B). Curcumin 4 was similar to curcumin extract in stimulating ALP in hBMSCs. BDC 3 gave a 1.2-fold increase in ALP activity that was significantly ( $p < 0.01$ ) greater than curcumin 4. hBMSCs treated with CyBDC 6 increased ALP activity by 1.2-fold that was greater than CyCurc 7 (i.e., 1.1-fold,  $p < 0.1$ ). CyBDC 6 was less potent than BDC 3 in stimulating ALP activity in hBMSCs. Water-soluble curcumin amino acid conjugates were generally more effective at stimulating ALP activity in hBMSCs. BisVal-BDC 1 gave a 1.2-fold increase in ALP activity similar to results obtained using BDC 3. BisVal-CyBDC 2 gave a 1.2-fold increase in ALP activity ( $p < 0.05$ ). Water-soluble BDC 1 and 2 stimulated greater ALP activity than water-soluble curcumins 5 and 8. The results showed that BDC and derivatives (i.e., 1, 2, 3, and 6) were more potent stimulators of ALP activity than curcumin and derivatives (i.e., 4, 5, 7, and 8). Based on the potency of 1 and 2 and increased water solubility and stability, BisVal-BDC 1 and BisVal-CyBDC 2 (Fig. 1C) were selected for further studies.

#### hBMSC differentiation with TCP and 1 or 2

Compounds 1 or 2 stimulated hBMSC osteogenic lineage commitment in the presence of osteoinductive TCP granules (i.e., 500–1000  $\mu\text{m}$  granules).<sup>4</sup> Compounds 1 or 2 (500 nM) administered to hBMSCs incubated with TCP granules (5 mg/mL) for 8 or 25 days showed marked osteogenic differentiation based on ALP activity. For hBMSCs, ALP activity increased linearly from 0 to 5 mg/mL of TCP granules. Accordingly, 5 mg/mL TCP granules were used in osteogenesis experiments.

hBMSCs incubated with 1 (500 nM) for 8 days provided a 1.2-fold increase in ALP activity compared to vehicle-treated cells (Fig. 2A). hBMSCs treated with 1 (500 nM) + TCP granules (5 mg/mL) increased ALP activity by 2.0-fold

after 8 days (significantly greater than TCP granules (1.4-fold,  $p < 0.05$ ) or 1 alone (1.2-fold,  $p < 0.01$ )). After 25 days, hBMSCs treated with 1 or TCP granules alone increased ALP activity 1.8-fold and 2.2-fold, respectively. hBMSCs incubated with 1 and TCP granules showed a 3.1-fold increase in ALP activity (significantly greater than 1 ( $p < 0.001$ ) or TCP granules alone ( $p < 0.001$ )). In hBMSCs, addition of 1 showed time-dependent osteogenesis based on ALP activity over 25 days that was enhanced by TCP granules.

In hBMSCs, 2 + TCP granules stimulated osteogenesis (Fig. 2B). In the presence of TCP granules (5 mg/mL), hBMSCs treated with 2 (500 nM) stimulated ALP activity 1.4-fold after 8 days and 2.1-fold after 25 days. This effect was not statistically different than the effect of 2 or TCP granules alone at either time point. In summary, 1 and 2 both stimulated ALP activity in the absence of TCP granules, but the effects of 1 were greater than 2 in the presence of TCP granules.

Treatment of hBMSCs with 1 (500 nM) for 8 days induced a 1.7-fold, 1.6-fold, and 4.1-fold increase in *Runx2*, *BMP2*, and *Osteocalcin*, respectively ( $p < 0.001$ ), compared to vehicle-treated cells (Fig. 3 and Supplementary Table S2). Treatment of hBMSCs with TCP granules alone (5 mg/mL) resulted in a 2.3-fold increase in *Runx2* ( $p < 0.01$ ) and a 4.7-fold increase in *BMP2* ( $p < 0.01$ ) compared to vehicle-treated cells. These results showed that either 1 alone or TCP granules alone could stimulate hBMSC osteogenic differentiation. However, greatest induction of osteogenic target genes for hBMSCs occurred in the presence of 1 and TCP granules (2.4-fold, 5.4-fold, 8.7-fold, and 6.3-fold increases in *Runx2*, *BMP2*, *Osteopontin*, and *Osteocalcin*, respectively ( $p < 0.001$ )). Effects of 1 and TCP granules on *Osteopontin* and *Osteocalcin* expression significantly exceeded the effect of 1 or TCP granules alone. To extend these studies, additional osteogenic biomarker quantification at 8- and 20-day hBMSC cultivation showed increases although each biomarker had its own time-dependent profile

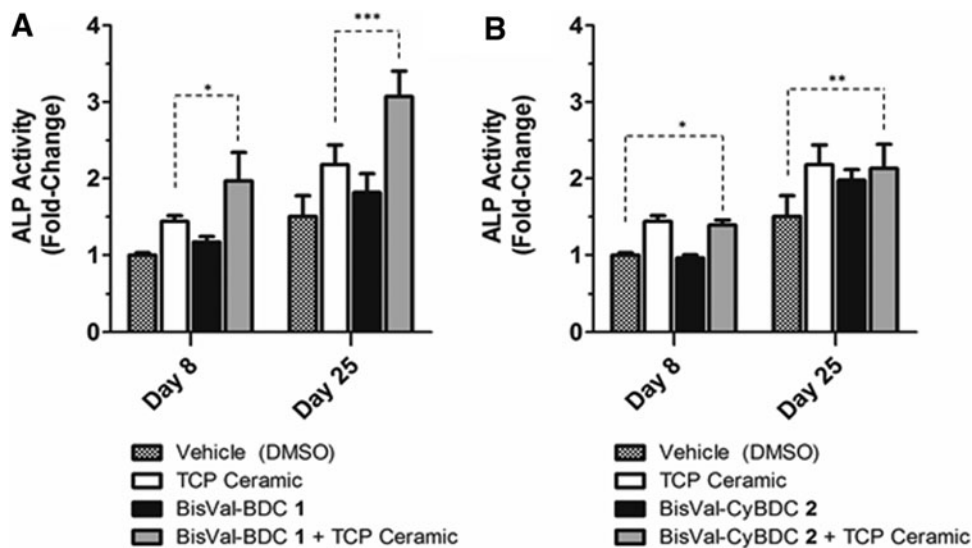


**FIG. 2.** Effect of 1 or 2 on alkaline phosphatase activity in hBMSCs incubated in the presence or absence of TCP granules. hBMSCs were incubated with compounds 1 or 2 (500 nM), TCP granules alone (5 mg/mL), or compounds 1 or 2 (500 nM) in the presence of TCP granules. ALP activity was measured after 8 and 25 days, and results were normalized to vehicle (i.e., DMSO)-treated cells on day 8. (A) ALP activity from hBMSCs treated with BisVal-BDC 1 in the presence or absence of TCP granules. (B) ALP activity from hBMSCs treated with BisVal-CyBDC 2 in the presence or absence of TCP granules. Data are mean  $\pm$  SD ( $n = 3$ ). \* $p < 0.05$ , \*\* $p < 0.01$ , \*\*\* $p < 0.001$ . TCP, tricalcium phosphate.

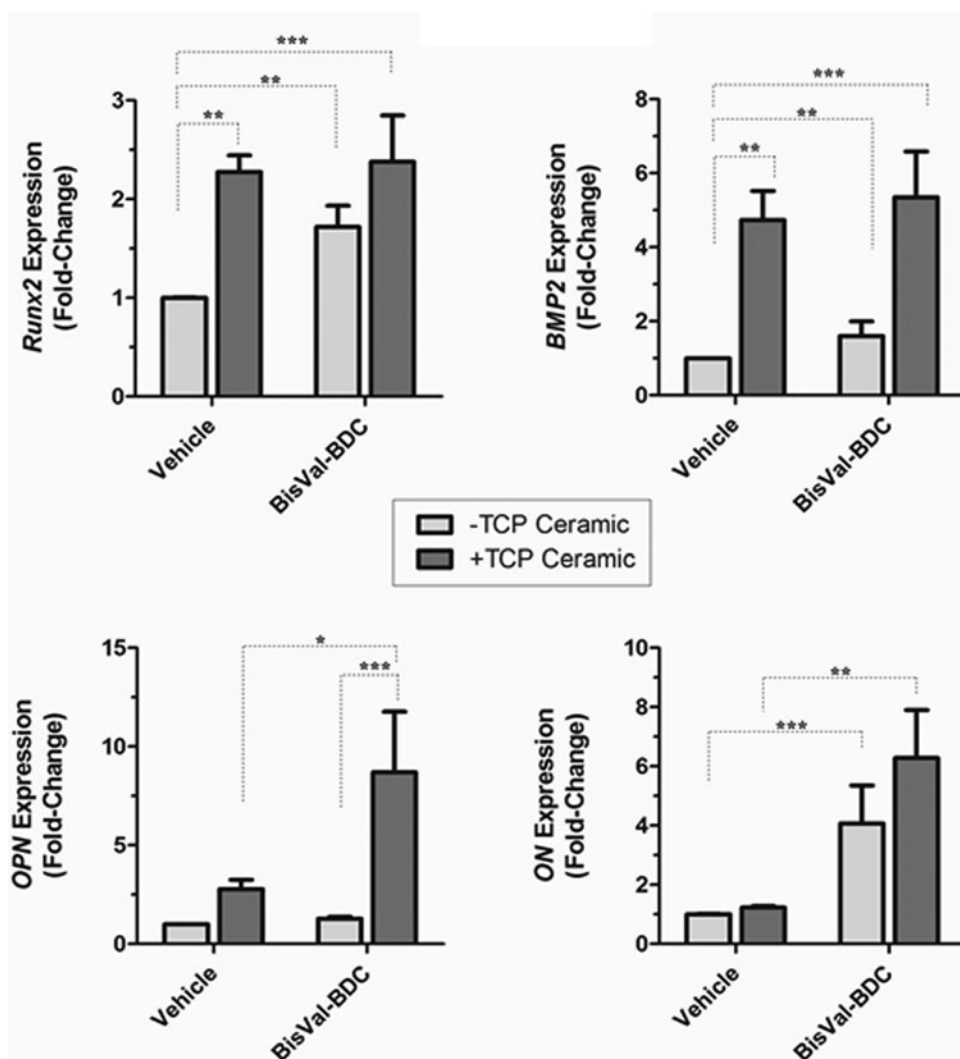


**FIG. 3.** Effect of 1 or 2 on osteogenic gene expression in hBMSCs incubated in the presence or absence of TCP granules. hBMSCs were incubated with compounds 1 or 2 (500 nM) and TCP granules (5 mg/mL). *Runx2*, *BMP2*, *OPN*, and *ON* gene expression was determined by qPCR after 8 days. Relative gene expression levels were normalized to vehicle (i.e., DMSO)-treated cells and expressed as fold-change in expression levels. Data were mean with error bars for SEM ( $n=4$ ). \* $p < 0.05$ , \*\* $p < 0.01$ , \*\*\* $p < 0.001$ .

(Supplementary Data). Results showed that administration of 1 and TCP granules to hBMSCs significantly induced osteogenic target gene expression. To confirm the PCR results, Western blot studies were done for cells treated for 8 days. Western blot analysis of cell extracts from 8-day cultivated cells treated with 1 (500 nM) + TCP (5 mg/mL) showed a 31-fold increase in immunoreactive ALP. As a control, a separate Western blot for cells treated with VD3 (500 nM) showed a 13-fold increase in immunoreactive ALP.

#### Effect of 1 or 2 on $Ca^{2+}$ deposition in hBMSCs

Accumulation of calcium is a biomarker of functional osteoblasts. Compared to vehicle-treated hBMSCs (Fig. 4A), 1 or 2 (500 nM) significantly increased Alizarin Red S calcium staining after 25 days of treatment (Fig. 4B, C). hBMSCs incubated with 1 or 2 + TCP granules (5 mg/mL) increased calcium deposition (Fig. 4D–F). Staining density quantification showed 1 and 2 increased calcium deposition in hBMSCs (2.0-fold), although analysis of staining in the presence of TCP granules was confounded by intrinsic calcium released from the ceramic (Fig. 4G, H). Results showed 1 or 2 to be equipotent for induction of calcium deposition in hBMSCs after 25 days in culture. In parallel, Oil Red O or

Alcian Blue staining of hBMSCs treated with 1 or 2 ± TCP granules at day 25 showed no apparent hBMSC differentiation to adipocytes or chondrocytes, respectively (Supplementary Figs. S1 and S2).

#### Effect of 1 or 2 on hBMSC viability

Cytotoxic effects of 1 or 2 (500 and 5000 nM) ± TCP granules were tested on hBMSCs *in vitro*. Gene expression for *Bax* and *c-Fos* that are upregulated in apoptosis showed that *Bax* and *c-Fos* were not detectable in any of the treatment groups as determined by qPCR. Cell viability of hBMSCs treated with 1 or 2 (500 nM and 5000 nM) ± TCP granules (5 mg/mL) measured by an Alamar Blue assay on day 25 showed no detectable decrease in cell viability compared to vehicle-treated hBMSCs. The results showed that *in vitro* differentiation of hBMSCs with curcumins ± TCP granules had no detrimental effects on the viability of hBMSCs.

#### Mechanistic studies of 1

Previously, we reported that small molecules modulate Wnt signaling and stimulate expression of *Runx2* and *BMP2* and promote osteogenesis.<sup>32</sup> The effect of curcumin 1 on expression of *Runx2* or *BMP2* and other target genes of

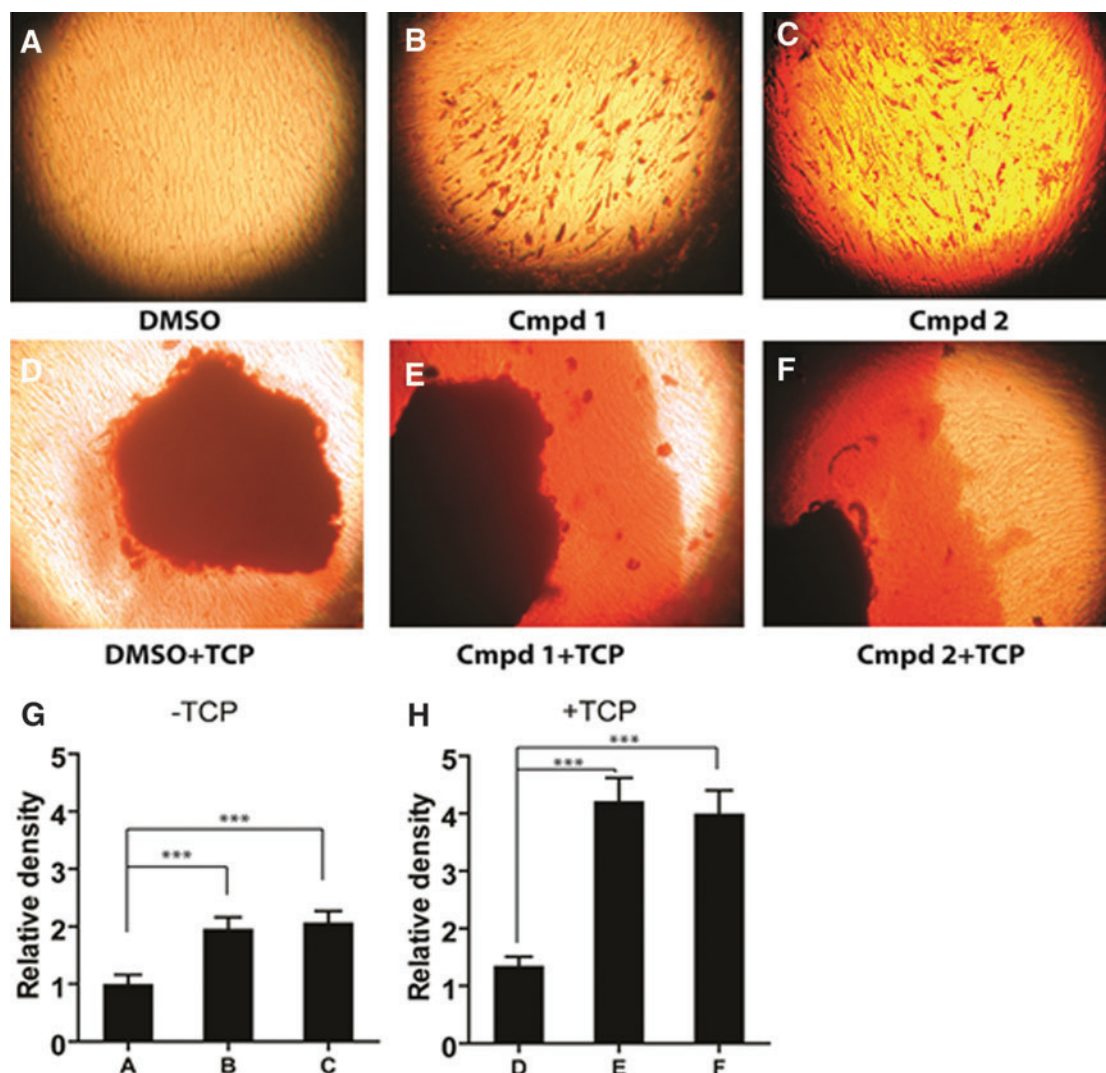


**FIG. 4.** Effect of 1 or 2 on  $\text{Ca}^{2+}$  Mineral Deposition in hBMSCs in the presence or absence of TCP granules. hBMSCs stained with Alizarin Red S after incubation with 1 or 2 (500 nM) in the presence or absence of TCP granules (5 mg/mL) for 25 days. Staining intensity in the images was quantified by densitometry and normalized to vehicle (i.e., DMSO)-treated cells. (A) Vehicle (i.e., DMSO)-treated cells. (B) BisVal-BDC 1. (C) BisVal-CyBDC 2. (D) TCP granules. (E) Compound 1 in the presence of TCP granules. (F) Compound 2 in the presence of TCP granules. (G) Densitometry analysis of (A–C) staining. (H) Densitometry analysis of (D–F) staining. Data are mean  $\pm$  SD ( $n=6$ ). \*\*\* $p<0.001$ . Color images are available online.

Wnt-mediated osteogenesis that showed administration of 1 alone to hBMSCs showed a 101-fold enhancement of *Runx2* (Fig. 5A). Coadministration of 1 and TCP granules showed an 8.2-fold increase in *Runx2* expression (Fig. 5A). Administration of 1 or TCP granules did not have as strong an effect on expression of *BMP2*, but 1 increased *BMP2* expression 7.5 fold in the presence of TCP granules (Fig. 5B). One stimulated *Runx2* expression in hBMSCs, while in the presence of TCP granules, 1 caused a synergistic increase in expression of *BMP2*.

Expression of Wnt-related genes *Axin2*, *Wnt3a*, *Wnt5a*, and *Sox9* was examined as biomarkers of Wnt-mediated hBMSC osteogenic differentiation. *Axin2* is a negative regulator of Wnt signaling. One (500 nM) or TCP granules (5 mg/mL) inhibited *Axin2* expression by 76% (Fig. 5C). Compound 1 or TCP granules alone did not significantly induce *Wnt3a* expression in hBMSCs, but 1 and TCP gran-

ules increased *Wnt3a* expression 62.3-fold (Fig. 5D). Thus, 1 plus TCP granules promoted *Wnt3a* and simultaneously inhibited expression of *Axin2*, a Wnt repressor gene. Administration of 1 to hBMSCs in the presence of TCP granules caused a 6.3-fold increase in *Wnt5a* expression (Fig. 5E). *Wnt5a* expression is an antiadipogenic biomarker in hBMSCs.<sup>33</sup> In hBMSCs, 1 plus TCP granules caused a 40% decrease in *Sox9* expression (Fig. 5F). *Sox9* expression is a chondrogenic biomarker.<sup>34</sup> Thus, 1 inhibited adipogenesis and chondrogenesis by inhibiting master regulatory genes in their respectful lineages.

#### Characterization of hBMSC-TCP implants

Based on the pharmaceutical properties and promising pharmacological properties of 1 plus TCP, we examined their ability to grow bone cells *in vivo*. A TCP-collagen

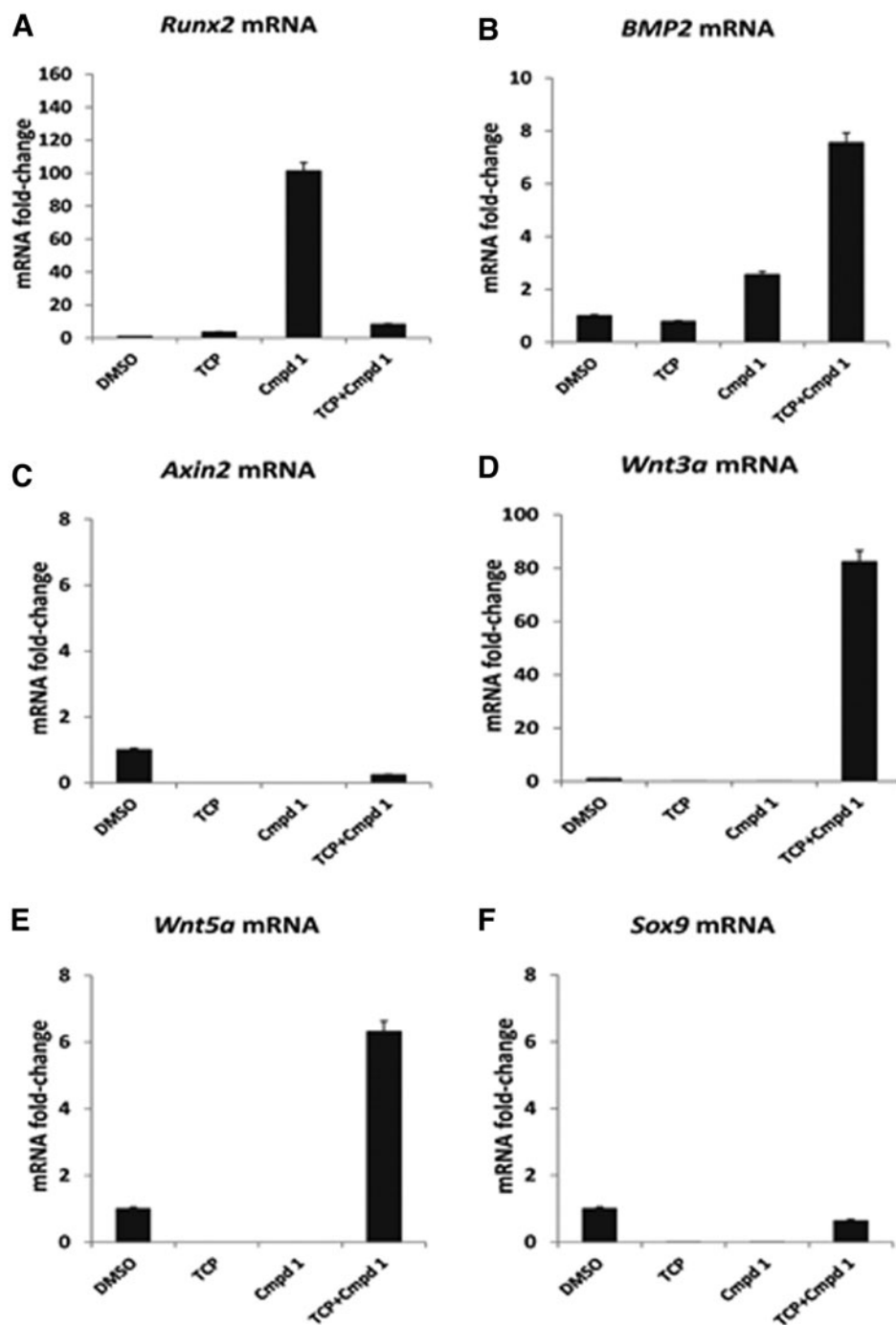


**FIG. 5.** Effect of compound 1 on induction of hBMSC Wnt gene expression in the presence or absence of TCP granules: Mechanistic studies. hBMSCs were incubated with compound 1 (500 nM) in the presence or absence of TCP granules (5 mg/mL), and expression of Wnt inducible target genes was determined after 8 days in culture by quantifying mRNA with qPCR. Gene expression was normalized to vehicle (i.e., DMSO)-treated cells. (A) *Runx2*, (B) *BMP2*, (C) *Axin 2*, (D) *Wnt3a*, (E) *Wnt5a*, (F) *Sox9*. Data are mean  $\pm$  SD ( $n = 3$ ).

scaffold that comprised 88% (wt/wt) TCP granules and 12% (wt/wt) bovine collagen I was used as a cell carrier scaffold for testing cell implants in an L4-L5 spinal fusion model in rats. Implants were designed to overlay on the dorsal aspect of a rat's vertebrae and extend 10 mm in total length to ensure extensive surface contacts with L4 and L5 transverse processes (Fig. 6A). The TCP scaffold had a 4-mm long projection designed to fill the void space between L4 and L5 transverse processes where fusion mass was desired. Average mass of the shaped TCP collagen scaffold was  $145 \pm 25$  mg and absorbed  $150 \mu\text{L}$  of an aqueous-cell solution. A radiograph of a rat that received bilateral 1-stimulated hBMSC implants of shaped TCP-collagen scaffold after

6 weeks is shown in Figure 6B. Greater than 95% of cells were adsorbed on a TCP-collagen scaffold after direct application of an hBMSC suspension in DMEM as determined by cell counting. Adsorbed hBMSCs remained viable on the TCP scaffold over the time frame of surgical implantation (i.e., <6 h) as shown by Live/Dead staining of implants (Fig. 6C). Results confirmed the presence of viable cells in implants used in spinal fusion experiments.

Excess hBMSCs that were not used in the *in vivo* studies (i.e., cells treated with 1 (500 nM) + TCP (5 mg/mL) or TCP alone) were used for another experiment. After 6 days of cultivation *in vitro*, excess hBMSCs that were not used in the *in vivo* fusion studies (Figs. 6 and 7) were cultured for an



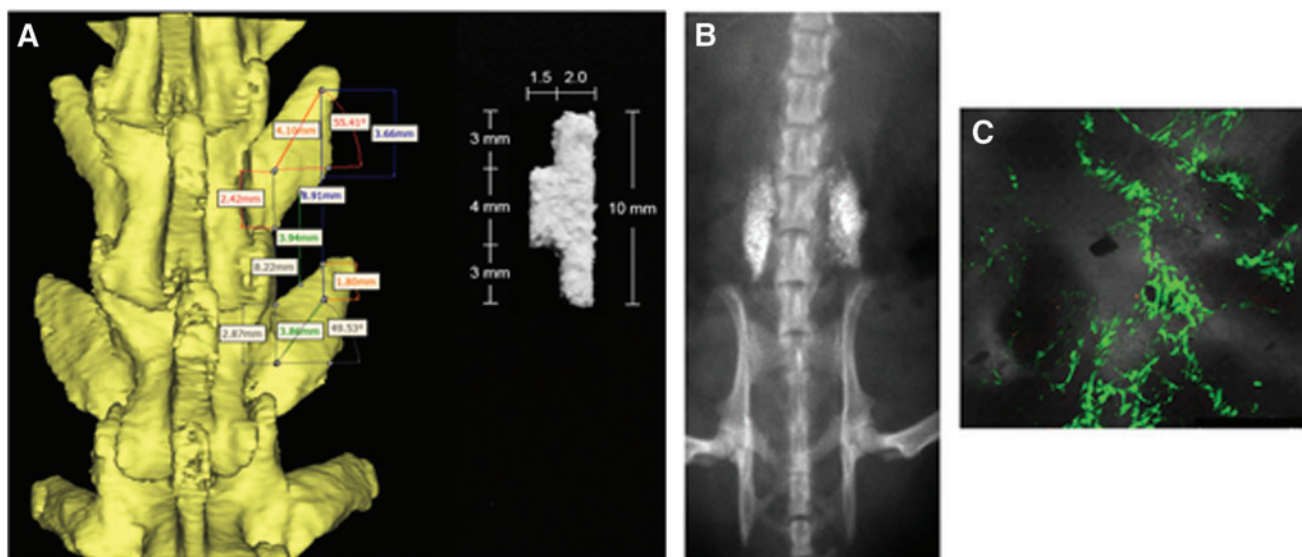


**FIG. 6.** TCP-collagen scaffold used for posterolateral spinal fusion. **(A)** Shaped TCP-collagen scaffolds were prepared with dimensions (millimeters) to fit the void space between L4 and L5 transverse processes using a  $\mu$ CT image of an adult rat lumbar spine as reference. **(B)** Representative 6-week radiograph of a rat that received bilateral BisVal-BDC (1)-stimulated hBMSC implants on the shaped TCP-collagen scaffold. **(C)** Confocal fluorescent microscopy image of compound 1-stimulated hBMSCs that were stained with Live-Dead Stain 6 h after adsorption of cells to the scaffold. Image taken at  $10\times$  magnification. Color images are available online.

additional 2 days in maintenance media ( $\alpha$ -MEM, 20% FBS, and  $1\times$  GlutaMAX) in the absence of any additional compound treatment. At the end of this 2-day period, cells were isolated and prepared for ALP functional activity as described herein. Compared to TCP alone treated cells, cells previously treated with 1 + TCP showed a  $1.2\pm 0.1$ -fold increase ( $p < 0.05$ ).

#### *Effect of 1-treated hBMSC-TCP scaffold implants in an immunodeficient rat model*

Compound 1-treated hBMSCs combined with TCP scaffold afforded implants that were compared to untreated hBMSC-TCP scaffold or TCP scaffold alone implants in a rat model of posterolateral spinal fusion. Previously, we determined that an 8-day *in vitro* incubation period gave significant osteogenic lineage commitment. Thus, 8-day cultivated cells were harvested, or media alone was adsorbed onto TCP-collagen scaffolds. Three groups of immunodeficient rats ( $n=7$ /group) received implants: (i) 1-stimulated hBMSC-TCP scaffold implants containing  $0.7\text{ M}$  cells, (ii) untreated hBMSC-TCP scaffold implants containing  $0.7\text{ M}$  cells, and (iii) TCP scaffold alone (i.e., no cells).

Following surgical implantation at L4 and L5 transverse processes, biweekly radiographs were taken. Weekly X-Ray time courses of spinal implants of animals analyzed with an exponential growth equation showed that 1-stimulated hBMSC-TCP scaffold implants, untreated hBMSC-TCP scaffold implants, and TCP scaffold alone (i.e., no cells) had a doubling time of  $0.54\pm 0.03$ ,  $0.5\pm 0.02$ , and  $0.53\pm 0.03$  weeks, respectively. After 8 weeks, the growth was not statistically significantly different among groups (Fishers information parameter ( $p\geq 0.05$ )). After 8 weeks rats were euthanized and analyzed further.

Intact rat lumbar spine segments (i.e., S4-L5) were removed from euthanized rats and analyzed for spinal fusion.

Visual analysis was done by blinded trained observers. Motion of implants was evaluated under constant bending force, and implants were ranked for fusion (i.e., secure fusion mass between transverse processes), partial fusion (i.e., fusion mass bridging transverse processes maintained, but some motion observed), or nonfusion (i.e., implants were unsecure or did not bridge the transverse processes). Cell implants were ranked as either fused or partially fused by 8 weeks (Fig. 7A). No statistically significant difference was observed between 1-treated hBMSC-TCP implants (65% fused, 35% partially fused) and untreated hBMSC-TCP implants (75% fused, 25% partially fused). However, both cell implants gave greater fusion than TCP alone implants (42% fusion, 42% partial fusion, and 12% nonfusion). Visual bending evaluation showed for 1-treated hBMSC-TCP scaffold implants, untreated hBMSC-TCP scaffold implants, and TCP scaffold alone implants (i.e.,  $0.36\pm 0.1$ ,  $0.25\pm 0.1$ , and  $0.71\pm 0.2$ , respectively) was not statistically significantly different (unpaired means comparison,  $p\geq 0.05$ ).

Accordingly, a more quantitative analysis of L4-L5 lateral bending of spine segments was done using three dimensional  $\mu$ CT disc height measurements as a quantitative spinal stability measure under constant bending forces.<sup>35</sup> Lumbar spinal segments (i.e., S1 to L1) were displaced in left lateral-bending ( $+10.0\text{ mm}$ ) and right lateral-bending ( $-10.0\text{ mm}$ ) positions from the neutral position for  $\mu$ CT disc height measurements using a custom radiopaque bending apparatus. Lateral displacement resulted in an average  $15^\circ$  bend in lumbar spines. Disc height deviation from the neutral position was determined by taking the sum of contraction and elongation of disc heights on left and right sides of the disc under lateral bending forces (Fig. 7B). Independent measurements from left and right bending were averaged to give disc height deviation from neutral position for each spinal segment. Using this quantifiable metric,

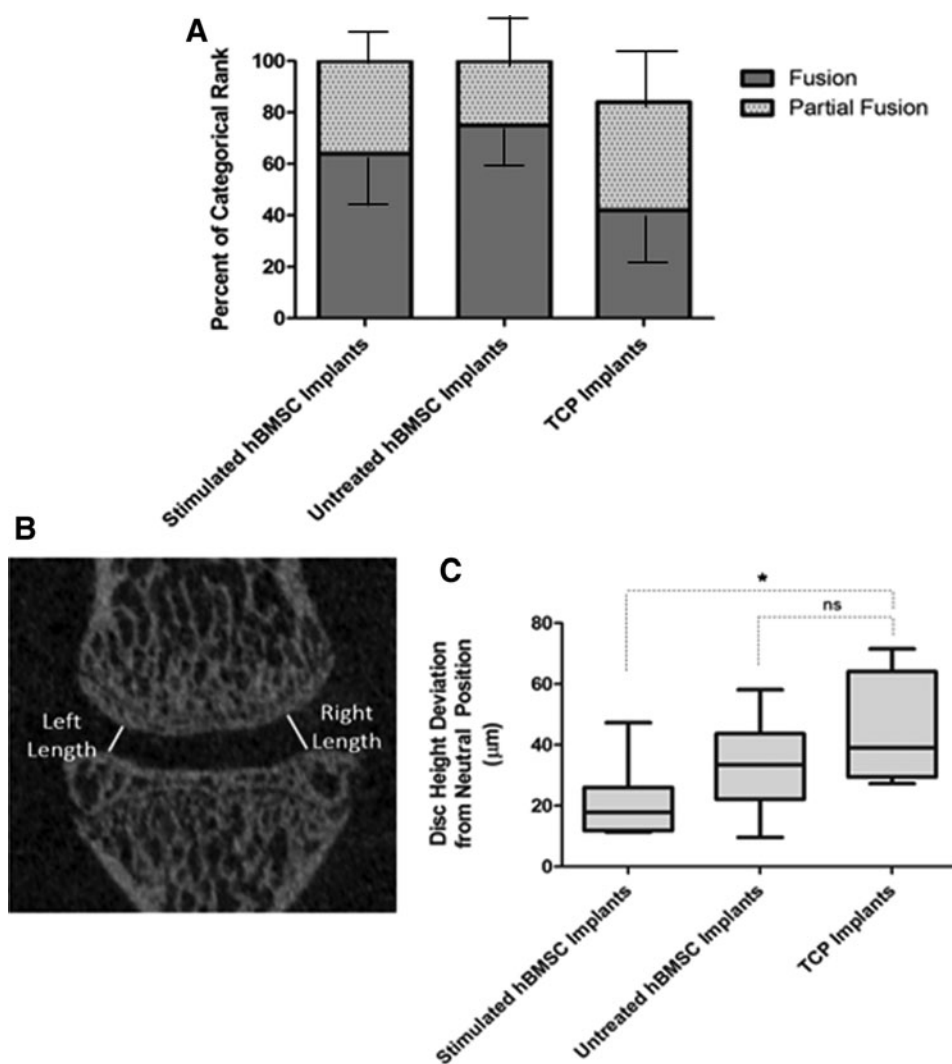


**FIG. 7.** Effect of implants on L4-L5 spinal fusion in spinal segments. **(A)** Removed rat spines containing implants were subjected to constant bending forces and visually ranked by blinded trained observers. Implants were ranked as fused (bridging, secure fusion mass), partially fused (bridging fusion mass that showed limited motion), or nonfused (not bridging or unsecure implants). Categorical rankings were expressed as a percent of the total number of animals in each group. **(B)** Representative  $\mu$ CT image of L4-L5 vertebral disc height measurements used for determining stability of the lumbar spinal segments under a controlled lateral displacement. The distance of the *left* length and *right* length of the L4-L5 disc height was determined by  $\mu$ CT at the neutral position and then under a constant *left* (+10 mm) and *right* (−10 mm) lateral displacement. Deviation in disc height was calculated from the averaged differences in disc height from the neutral position that represented the absolute sum of contraction and elongation deviations. **(C)** Quantification of absolute deviation in disc heights ( $\mu$ m) with constant lateral displacement shown in a Box and Whisker Plot with 75th percentile (*box*), minimum and maximum values (*whiskers*), and median (*line*) with  $n = 7$ /group. \*  $p < 0.05$ , ns = not significant (i.e.,  $p > 0.1$ ). Compound 1-treated hBMSC-TCP scaffold implants (stimulated hBMSC implants), nontreated hBMSC TCP scaffold implants (untreated hBMSC implants), and TCP scaffold implants were described above.

1-treated hBMSC-TCP scaffold implants showed the greatest stabilization of rat spinal segments at L4-L5 under lateral bending forces with an average total displacement from the neutral position of 22  $\mu$ m (Fig. 7C).

By comparison, untreated hBMSC-TCP scaffold implants showed greater deviation of disc heights under lateral bending forces with an average total displacement of 34  $\mu$ m. TCP scaffold alone implants gave an average of 44  $\mu$ m total disc height deviation that represented a two-fold greater deviation (i.e.,  $p < 0.05$ ) in disc height deviation compared to 1-treated hBMSC-TCP scaffold implants. Results showed

that 1-treated hBMSC-TCP scaffold implants achieved spinal fusion and provided greater stability of the spinal column than untreated hBMSC-TCP scaffold implants or TCP alone implants.<sup>36</sup>

Explants were analyzed for extent of bone formation by histology (Fig. 8). Nondecalcified histological sections (Goldner's Trichrome) were quantified by densitometry analysis to compare surface area of bone in sections of fusion mass. Compound 1-treated hBMSC TCP scaffold implants resulted in new bone tissue in 1% of total histological surface area of tissue sections examined, while much

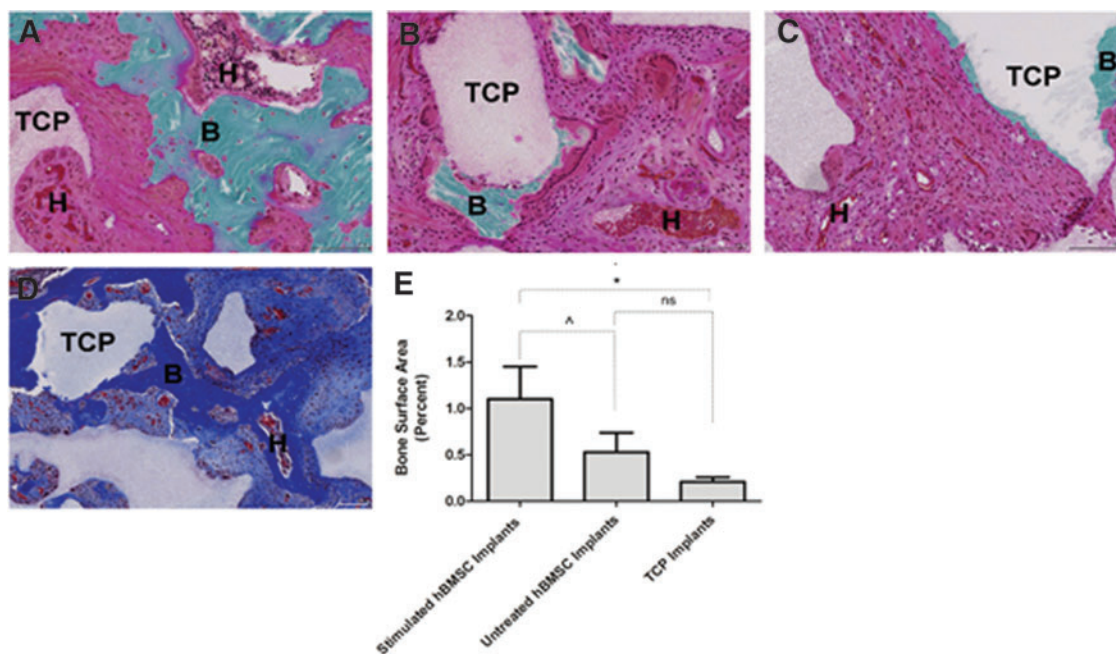


**FIG. 8.** Histology of L4-L5 fusion mass from implants (A–D). Representative histological sections labeled: B, bone; TCP, tricalcium phosphate; H, hematopoietic territories. Goldner’s Trichrome stained sections of (A). Compound 1-treated hBMSC-TCP scaffold implants (20 $\times$ ), (B). Untreated hBMSC-TCP scaffold implants (20 $\times$ ) and (C). TCP scaffold alone implants (i.e., no cells) (20 $\times$ ). (D). Masson’s Trichrome stained decalcified section of compound 1-stimulated hBMSC-TCP scaffold implants (10 $\times$ ). Scale bar = 100  $\mu$ m in images. (E). Quantitative densitometry analysis of *de novo* bone surface area in nondecalcified stained sections expressed as bone surface area as a percent of the total histological section. Data are the averaged values showing standard error of the mean ( $n=7$ /group). ^, almost significant; ns, not significant.  $p < 0.10$ , \* $p < 0.05$ . Color images are available online.

of the other tissue was a dense collagenous tissue that bone growth plates appeared to have emerged. Compound 1-treated hBMSC-TCP scaffold implants had 2.0-fold greater bone surface area in fusion mass than untreated hBMSC-TCP scaffold implants (0.5% surface area,  $p < 0.1$ ). Compound 1-treated hBMSC-TCP scaffold implants afforded 5.0-fold greater bone surface area in the fusion mass compared to TCP scaffold alone implants (0.2% surface area,  $p < 0.05$ ). This analysis specifically excluded regions of contiguous bone mass with the transverse processes that largely underestimated total new bone formation in implants (i.e., *de novo* bone tissue could not be definitively resolved against the transverse processes despite administration of fluorescent bone labels and was excluded from this analysis).

Greater bone formation associated with 1-treated hBMSC TCP scaffold implants manifested as contiguous growth plates that emerged from an amorphous tissue surrounding TCP scaffold. Residual TCP scaffold was observed to have incorporated osteoblasts on their periphery, but the scaffold themselves were not noticeably remodeled after 8 weeks. In addition to bone tissue, extensive hematopoietic territories in histological sections were observed that supported good biological integration of implants in all treatment groups, including the noncell group (i.e., TCP scaffold alone). No significant differences were found among treatment groups for hematopoietic territory surface area by densitometry analysis of histological sections. Overall, the histological results showed that spinal segments receiving 1-treated hBMSC-TCP scaffold implants provided more mature fusion mass and twice as much bone after 8 weeks compared to untreated hBMSC-TCP scaffold implants.

## Discussion

Curcuminoids can be used safely<sup>37,38</sup> to promote osteogenesis in hBMSCs. Curcumin and minor component BDC (i.e., 3, Fig. 1)<sup>25</sup> have been used safely for oncology, inflammation, and immune modulation.<sup>36</sup> BDC is more potent than curcumin in upregulation of certain genes, including vitamin D3.<sup>28,37</sup>

Comparison of BDC prodrug (i.e., 1) to BDC (3) showed that water-soluble prodrug 1 was a more potent inducer of hBMSC proliferation. Administration of 1 or 2 to hBMSCs promoted osteogenic differentiation *in vitro*, but in the presence of osteoinductive TCP granules, cell differentiation was markedly increased. Results with 1 and 2 contrast those of curcumin on rat MSCs that showed induction of ALP but only at elevated concentrations (i.e., 10–20  $\mu$ M).<sup>24</sup> 1 and 2 induced hBMSC osteogenic differentiation 20-fold greater than 4 likely due to increased solubility or stability/availability.<sup>38–40</sup> Prodrug 1 is a more potent inducer of hBMSC osteogenic differentiation than curcumin (3).

Previously, in C2C12 cells, we showed that small molecules induced *Runx2* and *BMP2* expression for synergistic osteogenic differentiation.<sup>32</sup> This is similar to cooperativity between Wnt and BMP2 signaling for osteogenic differentiation of hBMSCs.<sup>41–43</sup> In C2C12 cells, compared to BMP2 (100 ng/mL), compound 1 (500 nM)+TCP granules (5 mg/mL) was equal or superior to induction of gene markers *BMP2*, *ALP2*, *Col 1*, and *Runx2* (unpublished). Small molecule compound 1 may thus possess properties that simulate BMP2 but avoid adverse effects of BMP2.

In hBMSCs, 1 upregulates *Runx2*, *Wnt3a*, and *BMP2* and decreases expression of *Axin2* (a pro-adipogenic factor<sup>44,45</sup>) in

hBMSCs (Fig. 5). Compound 1 decreased *Sox9* (a chondrogenic factor in hBMSCs<sup>46,47</sup>). Thus, 1 inhibited both adipogenesis and chondrogenesis during promotion of osteogenesis in hBMSCs. While the molecular target of 1 is unknown, curcumin is an inhibitor of glycogen synthase kinase-3 $\beta$  (GSK-3 $\beta$ ).<sup>48,49</sup> Wnt activation by 1 extends the scope of curcumins that activate this signaling pathway. Compound 1 increased *TLR* expression during osteogenic differentiation. hBMSCs show a wide range of *TLR* expression.<sup>50</sup> *TLR4* stimulation is correlated with osteogenesis in hBMSCs, and *TLR3* stimulates adipogenesis.<sup>51</sup> Compound 1-treated hBMSCs increased cell migration and *TLR4* expression and may help explain osteogenic differentiation and migration of hBMSCs to TCP like the postulated roles of TLRs in chemotaxis.<sup>52</sup>

hBMSCs treated with 1 synergized osteogenesis of TCP.<sup>53</sup> Osteoinductive properties of TCP used herein correlated with microstructure of particle surface.<sup>4</sup> Protein binding might be an important factor in mediating osteoinduction whereby growth factors and morphogens adsorb onto the surface of TCP to promote osteogenesis<sup>54,55</sup> and provide a microenvironment for bone growth.<sup>56</sup> It is notable that compound 1 adheres to TCP granules very efficiently (nearly 100%), and this may contribute to the synergistic potency of the combination. Calcium release from TCP may also contribute to this microenvironment.<sup>57,58</sup> Stimulation of hBMSCs with 1 that modulates osteogenic signaling affords marked effects on cell fate and provides a novel approach to inducing cell differentiation. In contrast, TCP alone showed little effect on expression of Wnt target genes examined in this study.

hBMSCs have been cultured in the presence of osteogenic media<sup>31</sup> and combined with a carrier substance for transplantation.<sup>59-62</sup> Administration of dexamethasone to hBMSCs in osteogenic media before implantation resulted in improved bone formation.<sup>63</sup> Similarly, hBMSCs cultured with calcium phosphate microspheres and transplanted afforded improved bone formation in a mouse calvarial defect model.<sup>64</sup> Osteogenic media has not always provided improved bone growth following transplantation of cells,<sup>65</sup> and paradoxically, long-term effects of glucocorticoids *in vivo* led to promotion of bone loss.<sup>66</sup> Purmorphamine applied to hydroxyapatite discs increased bone formation after implantation.<sup>67</sup> Compound 1-treated hBMSCs grown in the presence of TCP granules can serve as a standalone replacement of osteogenic media. The advantage of this *ex vivo* cell model approach is that cells can then be placed onto a similar TCP scaffold microenvironment used in *in vitro* induction and implanted *in vivo*. Addition of 1 in the presence of TCP granules to osteogenic media (unpublished) showed greater stimulation of osteogenic markers. Taken together, results show that 1 with osteoinductive TCP granules was highly osteoinductive to hBMSCs.

Eight-day *ex vivo* induction of hBMSCs by 1 and TCP granules and then implantation on a TCP scaffold afforded osteoid-like tissue formation following implantation *in vivo*. hBMSCs induced with 1, implanted in rats, and analyzed 8 weeks later showed dense osteoid-like tissue present in induced cell implants that were generally lacking in implants from untreated cells. Progression to mature bone may require a longer time course.

In conclusion, 1 modulated osteogenesis of hBMSCs, including proliferation, differentiation, and mineralization. These effects were greatly enhanced when 1 was adminis-

tered to cells cultured in the presence of TCP granules. Administration of small-molecule 1 to hBMSCs in the presence of TCP to induce osteogenesis avoids challenges of systemic administration of small molecules or a biologic. This procedure may also be beneficial in a situation where stem cells originate from patients with risk factors or older age. Thus, findings reported herein represent a new strategy to prepare cell therapies for bone repair and regeneration.

### Acknowledgments

The authors thank Dr. Pam Robey of the National Institute of Health for hBMSC cells. The authors also thank Dr. Tim Moseley of NuVasive, Inc., (San Diego, CA) for the TCP granules and scaffold.

### Disclosure Statement

No competing financial interests exist.

### Funding Information

No external funding was received. Funding was from the Human BioMolecular Research Institute.

### Supplementary Material

Supplementary Data  
Supplementary Figure S1  
Supplementary Figure S2  
Supplementary Table S1  
Supplementary Table S2

### References

1. Betz, R.R. Limitations of autograft and allograft: new synthetic solutions. *Orthopedics* **25**, s561, 2002.
2. Pape, H.C., Evans, A., and Kobbe, P. Autologous bone graft: properties and techniques. *J Orthop Trauma* **24**, S35, 2010.
3. Holtzclaw, D., Toscano, N., Eisenlohr, L., and Callan, D. The safety of bone allografts used in dentistry: a review. *J Am Dent Assoc* **139**, 1192, 2008.
4. Yuan, H., Fernandes, H., Habibovic, P., *et al.* Osteoinductive ceramics as a synthetic alternative to autologous bone grafting. *Proc Natl Acad Sci U S A* **107**, 13614, 2010.
5. Bianco, P., Cao, X., Frenette, P.S., *et al.* The meaning, the sense and the significance: translating the science of mesenchymal stem cells into medicine. *Nat Med* **19**, 35, 2013.
6. Robey, P.G. Cell sources for bone regeneration: the good, the bad, and the ugly (but promising). *Tissue Eng B Rev* **17**, 423, 2011.
7. Bielby, R., Jones, E., and McGonagle, D. The role of mesenchymal stem cells in maintenance and repair of bone. *Injury* **38**, S26, 2007.
8. DiMarino, A.M., Caplan, A.I., and Bonfield, T.L. Mesenchymal stem cells in tissue repair. *Front Immunol* **4**, 201, 2013.
9. Ryan, J.M., Barry, F.P., Murphy, J.M., and Mahon, B.P. Mesenchymal stem cells avoid allogeneic rejection. *J Inflamm* **2**, 8, 2005.
10. Liu, H., Kemeny, D.M., Heng, B.C., Ouyang, H.W., Melendez, A.J., and Cao, T. The immunogenicity and immunomodulatory function of osteogenic cells differentiated from mesenchymal stem cells. *J Immunol* **176**, 2864, 2006.
11. Caplan, A.I., and Correa, D. The MSC: an injury drugstore. *Cell Stem Cell* **9**, 11, 2011.

12. Giordano, A., Galderisi, U., and Marino, I.R. From the laboratory bench to the patient's bedside: an update on clinical trials with mesenchymal stem cells. *J Cell Physiol* **211**, 27, 2007.
13. Blackwood, K.A., Bock, N., Dargaville, T.R., and Ann Woodruff, M. Scaffolds for growth factor delivery as applied to bone tissue engineering. *Int J Polym Sci* **2012**, 25, 2012.
14. Carragee, E.J., Hurwitz, E.L., and Weiner, B.K. A critical review of recombinant human bone morphogenetic protein-2 trials in spinal surgery: emerging safety concerns and lessons learned. *Spine J* **11**, 471, 2011.
15. Lanier, M., Schade, D., Willems, E., *et al.* Wnt inhibition correlates with human embryonic stem cell cardiomyogenesis: a structure-activity relationship study based on inhibitors for the Wnt response. *J Med Chem* **55**, 697, 2012.
16. Schmale, A.C., Hubner, R., Beller, M., Rolfs, A., and Frech, M.J. Small molecules in stem cell research. *Curr Pharm Biotechnol* **14**, 36, 2013.
17. Wu, X., Ding, S., Ding, Q., Gray, N.S., and Schultz, P.G. A small molecule with osteogenesis-inducing activity in multipotent mesenchymal progenitor cells. *J Am Chem Soc* **124**, 14520, 2002.
18. Darcy, A., Meltzer, M., Miller, J., *et al.* A novel library screen identifies immunosuppressors that promote osteoblast differentiation. *Bone* **50**, 1294, 2012.
19. Park, K.W., Waki, H., Kim, W.-K., *et al.* The small molecule phenamil induces osteoblast differentiation and mineralization. *Mol Cell Biol* **29**, 3905, 2009.
20. Zhao, J., Ohba, S., Komiyama, Y., Shinkai, M., Chung, U.-i., and Nagamune, T. Icarin: a potential osteoinductive compound for bone tissue engineering. *Tissue Eng A* **16**, 233, 2010.
21. Okada, M., Sangadala, S., Liu, Y., *et al.* Development and optimization of a cell-based assay for the selection of synthetic compounds that potentiate bone morphogenetic protein-2 activity. *Cell Biochem Funct* **27**, 526, 2009.
22. Aggarwal, B.B., Surh, Y.-J., and Shishodia, S. The molecular targets and therapeutic uses of curcumin in health and disease. New York, NY: Springer; 2007.
23. Mishra, S., and Palanivelu, K. The effect of curcumin (turmeric) on Alzheimer's disease: an overview. *Ann Indian Acad Neurol* **11**, 13, 2008.
24. Gu, Q., Cai, Y., Huang, C., Shi, Q., and Yang, H. Curcumin increases rat mesenchymal stem cell osteoblast differentiation but inhibits adipocyte differentiation. *Pharmacognosy Mag* **8**, 202, 2012.
25. Volak, L.P., Ghirmai, S., Cashman, J.R., and Court, M.H. Curcuminoids inhibit multiple human cytochromes P450, UDP-glucuronosyltransferase, and sulfotransferase enzymes, whereas piperine is a relatively selective CYP3A4 inhibitor. *Drug Metab Dispos* **36**, 1594, 2008.
26. Masoumi, A., Goldenson, B., Ghirmai, S., *et al.*  $1\alpha,25$ -dihydroxyvitamin D<sub>3</sub> interacts with curcuminoids to stimulate Amyloid- $\beta$  clearance by macrophages of alzheimer's disease patients. *J Alzheimer's Dis* **17**, 703, 2009.
27. Fiala, M., Liu, P.T., Espinosa-Jeffrey, A., *et al.* Innate immunity and transcription of MGAT-III and Toll-like receptors in Alzheimer's disease patients are improved by bisdemethoxycurcumin. *Proc Natl Acad Sci U S A* **104**, 12849, 2007.
28. Cashman, J.R., Gagliardi, S., Lanier, M., Ghirmai, S., Abel, K.J., and Fiala, M. Curcumins promote monocytic gene expression related to beta-amyloid and superoxide dismutase clearance. *Neurodegener Dis* **10**, 274, 2012.
29. Funk, J.L., Oyarzo, J.N., Frye, J.B., *et al.* Turmeric extracts containing curcuminoids prevent experimental rheumatoid arthritis. *J Nat Prod* **69**, 351, 2006.
30. Yuan, H., Van Den Doel, M., Li, S., Van Blitterswijk, C.A., De Groot, K., and De Bruijn, J.D. A comparison of the osteoinductive potential of two calcium phosphate ceramics implanted intramuscularly in goats. *J Mater Sci Mater Med* **13**, 1271, 2002.
31. Jaiswal, N., Haynesworth, S.E., Caplan, A.I., and Bruder, S.P. Osteogenic differentiation of purified, culture-expanded human mesenchymal stem cells in vitro. *J Cell Biochem* **64**, 295, 1997.
32. Chen, S., Ryan, D.A., Dwyer, M.A., and Cashman, J.R. Synergistic effect of Wnt modulatory small molecules and an osteoinductive ceramic on C2C12 cell osteogenic differentiation. *Bone* **67**, 109, 2014.
33. Nishizuka, M., Koyanagi, A., Osada, S., and Imagawa, M. Wnt4 and Wnt5a promote adipocyte differentiation. *FEBS Lett* **582**, 3201, 2008.
34. Akiyama, H. Control of chondrogenesis by the transcription factor Sox9. *Mod Rheumatol* **18**, 213, 2008.
35. Yamaguchi, T., Inoue, N., Sah, R.L., *et al.* Micro-computed tomography-based three-dimensional kinematic analysis during lateral bending for spinal fusion assessment in a rat posterolateral lumbar fusion model. *Tissue Eng C Methods* **20**, 578, 2014.
36. Fukui, D., Kawakami, M., Cheng, K., *et al.* Three-dimensional micro-computed tomography analysis for spinal instability after lumbar facetectomy in the rat. *Eur Spine J* **26**, 2014, 2017.
37. Ravindran, J., Subbaraju, G.V., Ramani, M.V., Sung, B., and Aggarwal, B.B. Bisdemethylcurcumin and structurally related hispolon analogues of curcumin exhibit enhanced prooxidant, anti-proliferative and anti-inflammatory activities in vitro. *Biochem Pharmacol* **79**, 1658, 2010.
38. Anand, P., Kunnumakkara, A.B., Newman, R.A., and Aggarwal, B.B. Bioavailability of curcumin: problems and promises. *Mol Pharm* **4**, 807, 2007.
39. Quitschke, W.W. Bioavailability and Metabolism of Curcuminoids. In: Diederich, M., and Noworyta, K., eds. *Natural Compounds as Inducers of Cell Death*. Dordrecht, Netherlands: Springer, 2012, p. 95.
40. Rachmawati, H. Curcumin nanoforms promise better therapeutic values. *Int J Res Pharm Sci* **4**, 211, 2013.
41. Rodriguez-Carballo, E., Ulsamer, A., Susperregui, A.R., *et al.* Conserved regulatory motifs in osteogenic gene promoters integrate cooperative effects of canonical Wnt and BMP pathways. *J Bone Miner Res* **26**, 718, 2011.
42. Phimphilai, M., Zhao, Z., Boules, H., Roca, H., and Franceschi, R.T. BMP signaling is required for RUNX2-dependent induction of the osteoblast phenotype. *J Bone Miner Res* **21**, 637, 2006.
43. Kim, H.N., Min, W.K., Jeong, J.H., *et al.* Combination of Runx2 and BMP2 increases conversion of human ligamentum flavum cells into osteoblastic cells. *BMB Reports* **44**, 446, 2011.
44. Liu, G., Vijayakumar, S., Grumolato, L., *et al.* Canonical Wnts function as potent regulators of osteogenesis by human mesenchymal stem cells. *J Cell Biol* **185**, 67, 2009.
45. Naito, M., Mikami, Y., Takagi, M., and Takahashi, T. Up-regulation of Axin2 by dexamethasone promotes adipocyte



- differentiation in ROB-C26 mesenchymal progenitor cells. *Cell Tissue Res* **354**, 761, 2013.
46. Cheng, A., and Genever, P.G. SOX9 determines RUNX2 transactivity by directing intracellular degradation. *J Bone Miner Res* **25**, 2680, 2010.
  47. Giuliani, N., Lisignoli, G., Magnani, M., *et al.* New insights into osteogenic and chondrogenic differentiation of human bone marrow mesenchymal stem cells and their potential clinical applications for bone regeneration in pediatric orthopaedics. *Stem Cells Int* **2013**, 11, 2013.
  48. Ahn, J., Lee, H., Kim, S., and Ha, T. Curcumin-induced suppression of adipogenic differentiation is accompanied by activation of Wnt/beta-catenin signaling. *Am J Physiol Cell Physiol* **298**, C1510, 2010.
  49. Zhang, X., Yin, W.K., Shi, X.D., and Li, Y. Curcumin activates Wnt/beta-catenin signaling pathway through inhibiting the activity of GSK-3beta in APP<sup>sw</sup> transfected SY5Y cells. *Eur J Pharm Sci* **42**, 540, 2011.
  50. Delarosa, O., Dalemans, W., and Lombardo, E. Toll-like receptors as modulators of mesenchymal stem cells. *Front Immunol* **3**, 182, 2012.
  51. Waterman, R.S., Tomchuck, S.L., Henkle, S.L., and Betancourt, A.M. A new mesenchymal stem cell (MSC) paradigm: polarization into a pro-inflammatory MSC1 or an immunosuppressive MSC2 phenotype. *PLoS One* **5**, e10088, 2010.
  52. DelaRosa, O., and Lombardo, E. Modulation of adult mesenchymal stem cells activity by toll-like receptors: implications on therapeutic potential. *Mediators Inflamm* **2010**, 865601, 2010.
  53. Barradas, A.M., Yuan, H., van Blitterswijk, C.A., and Habibovic, P. Osteoinductive biomaterials: current knowledge of properties, experimental models and biological mechanisms. *Eur Cells Mater* **21**, 407, 2011.
  54. Jin, Q.M., Takita, H., Kohgo, T., Atsumi, K., Itoh, H., and Kuboki, Y. Effects of geometry of hydroxyapatite as a cell substratum in BMP-induced ectopic bone formation. *J Biomed Mater Res* **51**, 491, 2000.
  55. Kang, Y., Kim, S., Khademhosseini, A., and Yang, Y. Creation of bony microenvironment with CaP and cell-derived ECM to enhance human bone-marrow MSC behavior and delivery of BMP-2. *Biomaterials* **32**, 6119, 2011.
  56. Kang, Y., Kim, S., Bishop, J., Khademhosseini, A., and Yang, Y. The osteogenic differentiation of human bone marrow MSCs on HUVEC-derived ECM and beta-TCP scaffold. *Biomaterials* **33**, 6998, 2012.
  57. Barradas, A.M., Fernandes, H.A., Groen, N., *et al.* A calcium-induced signaling cascade leading to osteogenic differentiation of human bone marrow-derived mesenchymal stromal cells. *Biomaterials* **33**, 3205, 2012.
  58. Wang, Y.-K., and Chen, C.S. Cell adhesion and mechanical stimulation in the regulation of mesenchymal stem cell differentiation. *J Cell Mol Med* **17**, 823, 2013.
  59. Krebsbach, P.H., Kuznetsov, S.A., Satomura, K., Emmons, R.V.B., Rowe, D.W., and Robey, P.G. Bone formation in vivo: comparison of osteogenesis by transplanted mouse and human marrow stromal fibroblasts. *Transplantation* **63**, 1059, 1997.
  60. Mankani, M.H., Kuznetsov, S.A., Fowler, B., Kingman, A., and Ghebron Robey, P. In vivo bone formation by human bone marrow stromal cells: effect of carrier particle size and shape. *Biotechnol Bioeng* **72**, 96, 2001.
  61. Mankani, M.H., Kuznetsov, S.A., Marshall, G.W., and Robey, P.G. Creation of new bone by the percutaneous injection of human bone marrow stromal cell and HA/TCP suspensions. *Tissue Eng A* **14**, 1949, 2008.
  62. Eniwumide, J.O., Yuan, H., Cartmell, S.H., Meijer, G.J., and de Bruijn, J.D. Ectopic bone formation in bone marrow stem cell seeded calcium phosphate scaffolds as compared to autograft and (cell seeded) allograft. *Eur Cells Mater* **14**, 30, 2007.
  63. Song, I.H., Caplan, A.I., and Dennis, J.E. In vitro dexamethasone pretreatment enhances bone formation of human mesenchymal stem cells in vivo. *J Orthop Res* **27**, 916, 2009.
  64. Jin, G.-Z., Kim, J.-H., Park, J.-H., Choi, S.-J., Kim, H.-W., and Wall, I. Performance of evacuated calcium phosphate microcarriers loaded with mesenchymal stem cells within a rat calvarium defect. *J Mater Sci Mater Med* **23**, 1739, 2012.
  65. Kuznetsov, S.A., Mankani, M.H., and Robey, P.G. In vivo formation of bone and haematopoietic territories by transplanted human bone marrow stromal cells generated in medium with and without osteogenic supplements. *J Tissue Eng Regen Med* **7**, 226, 2013.
  66. Kim, C.H., Cheng, S.L., and Kim, G.S. Effects of dexamethasone on proliferation, activity, and cytokine secretion of normal human bone marrow stromal cells: possible mechanisms of glucocorticoid-induced bone loss. *J Endocrinol* **162**, 371, 1999.
  67. Gellynck, K., Shah, R., Parkar, M., Young, A., Buxton, P., and Brett, P. Small molecule stimulation enhances bone regeneration but not titanium implant osseointegration. *Bone* **57**, 405, 2013.

Address correspondence to:

John Cashman, PhD  
Human BioMolecular Research Institute  
5310 Eastgate Mall  
San Diego, CA 92121  
USA

E-mail: [jcashman@hbri.org](mailto:jcashman@hbri.org)

Received: July 24, 2020

Accepted: October 9, 2020

Online Publication Date: November 13, 2020